Catalyst size dependent growth of Pd-catalyzed one-dimensional InAs nanostructures

Hong-Yi Xu, Ya-Nan Guo, Zhi-Ming Liao, Wen Sun, Qiang Gao, Hark Hoe Tan, Chennupati Jagadish, and Jin Zou

Citation: Applied Physics Letters **102**, 203108 (2013); doi: 10.1063/1.4807597
View online: http://dx.doi.org/10.1063/1.4807597
View Table of Contents: http://scitation.aip.org/content/aip/journal/apl/102/20?ver=pdfcov
Published by the AIP Publishing

Catalyst size dependent growth of Pd-catalyzed one-dimensional InAs nanostructures

Hong-Yi Xu,[1] Ya-Nan Guo,[1] Zhi-Ming Liao,[1] Wen Sun,[1] Qiang Gao,[2] Hark Hoe Tan,[2] Chennupati Jagadish,[2] and Jin Zou[1,3,a)]
[1]*Materials Engineering, The University of Queensland, St Lucia, QLD 4072, Australia*
[2]*Department of Electronic Materials Engineering, Research School of Physics and Engineering, The Australian National University, Canberra, ACT 0200, Australia*
[3]*Centre for Microscopy and Microanalysis, The University of Queensland, St Lucia, QLD 4072, Australia*

(Received 25 April 2013; accepted 8 May 2013; published online 21 May 2013)

In this study, Pd was used as catalyst to grow one-dimensional InAs nanostructures on GaAs $(111)_B$ substrates in order to explore the growth mechanism and the effect of non-gold catalysts in growing epitaxial III-V nanostructures. With detailed morphological, structural, and chemical characterizations using electron microscopy, coupled with analysis of the Pd-In binary phase diagram, it was found that size of Pd nanoparticles plays a key role in determining the growth mechanism of one-dimensional InAs nanostructures. © *2013 AIP Publishing LLC*.
[http://dx.doi.org/10.1063/1.4807597]

One dimensional semiconductor nanostructures, particularly nanowires, have shown great potential in a wide range of applications in optoelectronics and nanoelectronics.[1–3] Among them, III-V nanostructures have become popular candidates due to their direct bandgaps,[4] high carrier mobility,[5] and high photoluminescence efficiency.[6,7] In order to realize and deliver the great potential of one dimensional III-V nanostructures, tremendous efforts have been devoted to their fabrication with improved morphological and crystallographic qualities using various techniques.[8–10] Most importantly, understanding the growth mechanisms of III-V nanowires is the key to improve their electronic and optical properties.

Epitaxial III-V nanowires are commonly grown in metal-organic chemical vapor deposition (MOCVD)[11,12] or molecular beam epitaxy systems[13,14] using Au as the catalyst,[15,16] because of its chemical inertness and ability to form eutectic with group III material at relatively low temperatures. In an MOCVD system, the morphological and crystal properties of the III-V nanowire are commonly controlled by tuning the growth temperature, V/III ratio, and precursor flow rate.[17–19] Recently, efforts have been devoted to controlling nanowire growths by varying the properties of the catalysts.[20,21] It has been demonstrated by controlling the shape of Au catalysts, the growth kinetics of InAs nanowires can be enhanced.[22] Furthermore, by tuning the phase of Ag-Au alloy catalysts, atomically sharp interfaces in Si/Ge nanowires can be realized.[23] Non-Au catalysts, such as Al,[24] Cu,[25] and Pd,[26,27] have also been effectively utilized to catalyze nanowire growth and to study the growth mechanisms of semiconductor nanowires. However, achieving high-quality III-V nanowire growth using non-Au catalysts remains challenging and requires further investigations to understand the fundamental growth mechanism.

In this letter, we demonstrate the growth of two kinds of one-dimensional InAs nanostructures using thin Pd film (developed into Pd particles with different sizes after annealing) as catalysts. Through detailed electron microscopy investigations, it has been found that high-quality InAs nanowires were grown via the vapor-liquid-solid (VLS) mechanism,[28] while InAs nanorods were grown via the vapor-solid-solid (VSS) mechanism.[24] The physical reasons of this observation have been discussed.

Prior to the nanostructure growth, a thin Pd film of 2 nm was deposited onto GaAs $\{111\}_B$ substrates in an electron-beam evaporator. The Pd coated substrate was then placed in the MOCVD chamber and annealed at 600 °C for 10 min under AsH_3 ambient to desorb surface contaminants and, more importantly, to agglomerate the Pd thin film into nanoparticles via Oswald ripening.[29] Trimethylindium (TMIn) was used as the group III precursor, while arsine (AsH_3) was used as the group V precursor for the nanostructure growth. The pressure of the growth chamber was stabilized at 100 millibars while the total input gas flow rate was 15 slm. The flow rates of TMIn and AsH_3 were 1.16×10^{-5} and 3.35×10^{-5} mol/min, respectively, resulting in a V/III ratio of 2.9. Based on previous studies and the binary In-Pd phase diagram,[30] the growth temperature was set at 500 °C. The morphological characteristics of InAs nanostructures and their corresponding catalysts were investigated by scanning electron microscopy (SEM, JEOL 7001F and JEOL 7800F, both operated at 15 kV) and their structural and chemical characteristics were investigated by transmission electron microscopy [TEM, Philips Tecnai F20, operated at 200 kV, equipped with energy dispersive spectroscopy (EDS) to determine the chemical compositions]. Individual nanowires were lifted off by using a sonicator and then transferred onto holey carbon films supported by Cu grids for TEM analyses.

Figure 1 is the typical SEM images of the nanostructures and show two different one-dimensional structures, namely the long inclined nanowires and short kinked nanorods. Figure 1(a) is a plan-view SEM image which shows a low density of nanowires that are straight and inclined with slightly tapered side-wall facets and a high density of

a)Email: j.zou@uq.edu.au

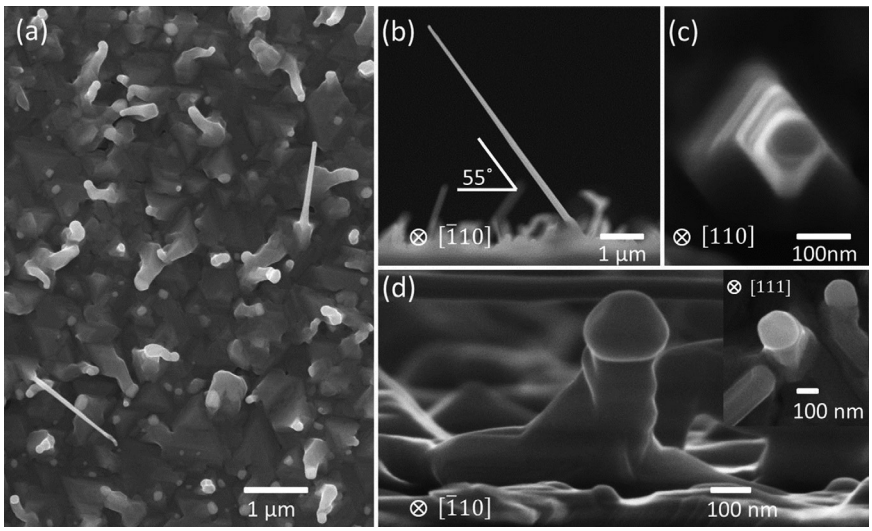

FIG. 1. (a) SEM overview of the Pd-catalyzed InAs nanostructures (top-view). (b) Side-view of a typical InAs nanowire. (c) A typical InAs nanowire viewed along the [110] direction (when the beam is parallel to the nanowire growth direction), showing the diamond shaped {111} sidewall facets of the nanowire. (d) Side view of a typical InAs nanorod. The inset is top-view of a typical InAs nanorod.

nanorods that are short and randomly kinked with a larger overall diameter than the nanowires. Figure 1(b) is a side-view SEM image taken from naturally cleaved sample (note that GaAs cleavage planes are {110} atomic planes) where the electron beam is parallel to the GaAs substrate surface. From this figure, an inclined nanowire is seen. According to our previous study,[27] these inclined nanowires grew along the $\bar{1}\bar{1}0$ directions with diamond shaped four {111} sidewall facets, as shown in Fig. 1(c) in which the SEM sample was tilted so that the electron beam was parallel to a ⟨110⟩ direction. On the other hand, the InAs nanorods are randomly kinked and do not grow along any particular crystallographic directions. The facets of the nanorod are also irregular due to the kinks and random growth directions [refer to Fig. 1(a)]. Fig. 1(d) is a magnified SEM image to show a typical nanorod with a faceted catalyst (with a size of ∼120 nm) on its top. Our extensive SEM investigation indicates that the size of the catalysts found on the nanorods always exceeds 100 nm in size [also refer to the inset of Fig. 1(d)], which is almost 3 times larger than that of the nanowire catalysts. We propose that the size differences of the catalysts may play a key role to reveal the growth mechanisms of both one-dimensional InAs nanostructures.

To clarify the role of Pd catalysts in the growth of InAs nanowires and nanorods, the chemical compositions of nanowires and nanorods, as well as their corresponding post-growth catalysts, were determined by EDS. Figures 2(a) and 2(f) are bright-field (BF) TEM images of a typical nanorod and a typical nanowire section near the tip, and Figs. 2(b) and 2(g) are their corresponding EDS spectra taken from the catalysts and the nanowire/nanorod, respectively. As can be seen, the post-growth catalyst on the top of the nanorod is faceted while the nanowire catalyst has a hemispherical shape. The quantitative analysis of EDS indicates that the two catalysts have identical chemical composition of ∼52 at. % Pd and ∼48 at. % In, while the compositions of the nanowire and nanorod are confirmed to be pure InAs (note that Cu peaks shown in EDS spectra are due to the Cu TEM

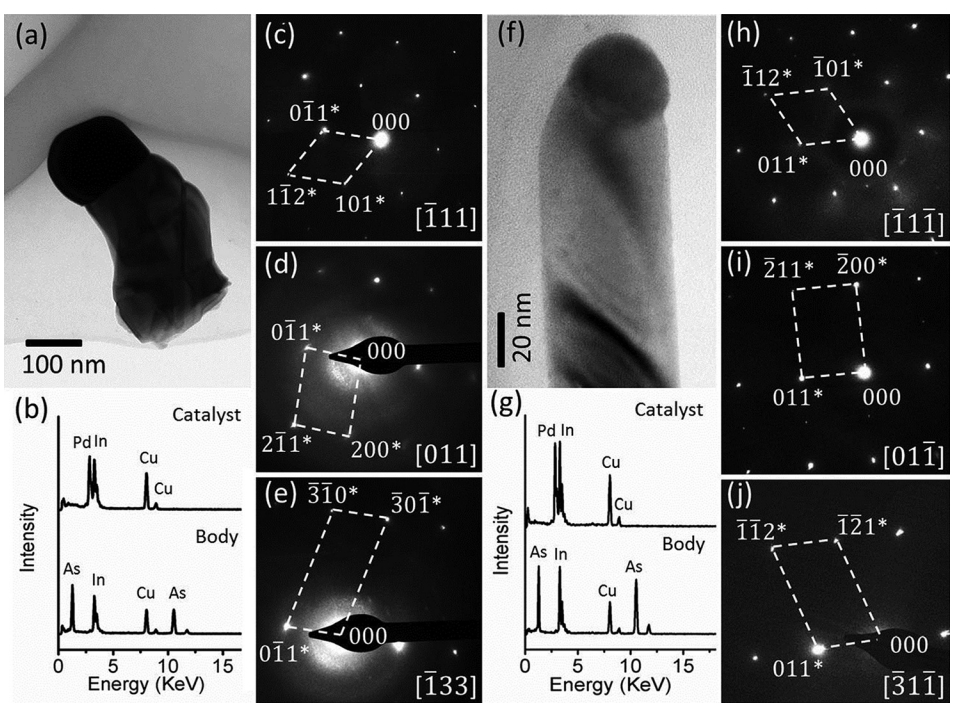

FIG. 2. (a) A BF TEM image of a typical nanorod. (b) EDS spectra taken at the catalyst and body regions of a typical Pd catalyzed nanorod. (c)–(e) SAED patterns of the nanorod catalyst taken along [$\bar{1}$11], [011], and [$\bar{1}$33] zone axes, respectively. (f) A BF TEM image of a typical nanowire near the catalyst. (g) EDS spectra taken at the catalyst and body regions of a typical Pd catalyzed nanowire. (h)–(j) SAED patterns of the nanowire catalyst taken along [$\bar{1}\bar{1}\bar{1}$], [01$\bar{1}$], and [$\bar{3}$1$\bar{1}$] zone axes, respectively.

grids). Furthermore, the crystal structures of both catalysts were carefully determined using selected area electron diffraction (SAED). Figures 2(c)–2(e) are SAED patterns taken from the nanorod catalyst shown in Fig. 2(a) along $\langle\bar{1}11\rangle$, $\langle 011\rangle$, and $\langle\bar{1}33\rangle$ zone axes. From these SAED patterns, the crystal structure of the nanorod catalyst can be determined as the body-center-cubic (BCC) phase of InPd with $a = 3.25$ Å (JCPDS No. 65-4804). On the other hand, Figures 2(h)–2(j) are the SAED patterns taken from the nanowire catalyst along $\langle\bar{1}1\bar{1}\rangle$, $\langle 01\bar{1}\rangle$, and $\langle\bar{3}1\bar{1}\rangle$ zone axes, from which its crystal structure can also be determined to be the same BCC structured InPd phase. It should be noted that both EDS and SAED studies suggest that the post-growth catalysts for both the nanorod and nanowire have an identical crystal structure with identical composition.

To understand why different size of catalysts lead to different forms (solid or liquid) of catalysts, we investigate the thin Pd film deposited on the GaAs $\{111\}_B$ substrate prior to the MOCVD growth. Figure 3(a) is a high magnification SEM image and shows that the thin film surface is rough, which can also be confirmed by cross-section TEM investigation. Figure 3(b) is such an example, where island surface is seen. Nevertheless, the mean thickness of the Pd thin film is confirmed to be ~2 nm by high-resolution cross-section TEM investigation [refer to Fig. 3(c)] with EDS analysis [refer to Fig. 3(d)]. It should be mentioned that the Ga and As peaks detected from the Pd thin film are generated from the GaAs substrate due to the thin Pd film. Based on these observations, we believe that, during the annealing process in the MOCVD reactor, uneven Pd thin film will develop into particles of different sizes due to Ostwald ripening.[31] Based on the fact that, after the growth, the sizes of the catalysts are significantly different, namely larger catalysts are faceted while smaller catalysts are hemispherical; we propose that the size of the catalysts plays a critical role during growth. As the surface to volume ratio increases rapidly with decreasing the catalyst size, the ability of precursors to diffuse into the smaller

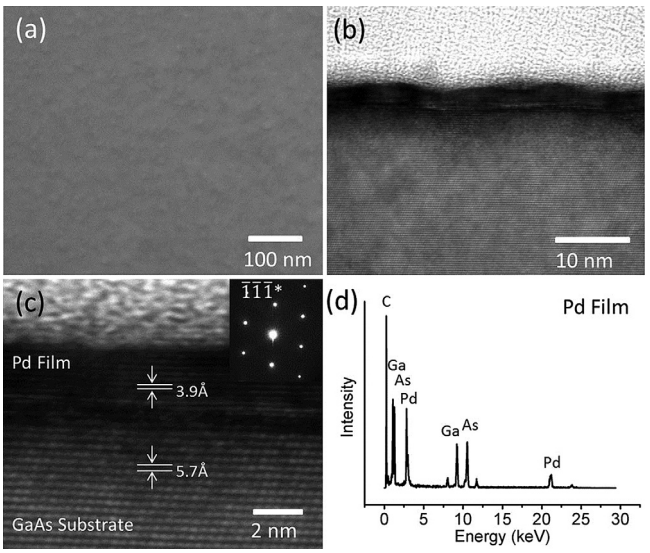

FIG. 3. (a) Top-view SEM image of the substrate coated with the Pd thin film before growth. (b) XTEM image of the thin Pd film and substrate before growth. (c) High resolution XTEM image of the thin Pd film. (d) EDS spectrum taken from the Pd thin.

catalysts is substantially enhanced.[32–34] As a consequence, the In concentration in the smaller Pd catalysts should be much higher than that in the larger catalysts during the growth. According to the In-Pd binary phase diagram,[30] with increasing In concentration in the In-Pd alloy, the melting temperature of the alloy decreases significantly ($T_m \approx 1285\,^{\circ}C$ at 48 at. % In, $T_m \approx 600\,^{\circ}C$ at 90 at. % In). Therefore, we anticipate that the smaller catalysts with higher In concentration could be in the liquid form during the growth, as opposed to those larger catalysts with lower In concentration, which are in the solid form during the growth. This argument is supported by our SEM and TEM observations, where smaller catalysts at the tip of the nanowires have a spherical shape while larger catalysts on tips of the nanorods have well-developed facets. Furthermore, we note that the In concentration in the InPd phase is very stable throughout its entire compositional range due to its low chemical potential.[35] The fact that the chemical compositions of post-growth catalysts of both nanowires and nanorods are identical suggests that In might be expelled from the smaller catalysts to reach the stable BCC In-Pd phase when the nanowire growth was terminated. Evidently, a "necking" phenomenon is observed in all nanowires [refer to Fig. 2(f)],[36] while such a "necking" cannot be seen in the nanorods with large and faceted catalysts [refer to Fig. 2(a)].

Based on our comprehensive SEM and TEM investigations, a growth model of Pd-induced InAs nanostructures can be schematically illustrated in Fig. 4. During the annealing stage, the deposited thin Pd film is broken down and agglomerated into Pd particles of different sizes under As-rich ambient. When the growth was initiated by switching on the TMIn, the Pd nanoparticles continuously absorbed In from the vapor to form Pd-In alloy. For smaller nanoparticles in the range of 30 nm or less, they may absorb a large amount of In to form liquid droplets due to the larger surface-to-volume ratio, while for larger Pd particles (exceeding 100 nm in size), the concentration of absorbed In is much lower and hence the nanoparticles remain solid at the growth temperature according to the Pd-In phase diagram (shown in Fig. 4). Therefore, in the case of small Pd catalysts, classical VLS growth model applies,[28] while for larger Pd particles, VSS growth model applies,[24] in which In atoms in the vapor diffuse through the solid catalysts to participate in the nanorod growth. Due to the slow diffusion rate of In atoms in the solid Pd catalysts and longer nucleation time of InAs crystals, the growth rate of the nanorods is slower than that of the nanowires. Furthermore, it should be mentioned that a clear nanorod/catalyst interface could not be identified through our extensive TEM investigations in over half a dozen nanorods, suggesting the catalyst was indeed in the solid form during the growth of the InAs nanorods, while the nanowire/catalyst interface was found to be $\{\bar{1}\bar{1}\bar{3}\}$, suggesting that the Pd catalysts were in the liquid form during the nanowire growth. More importantly, according to the In-Pd phase diagram and our experimental results, group III concentration in the catalyst alloy can effectively reduce its melting temperature to promote VLS growth. This sheds a light on using non-Au catalysts to promote nanowire growth even when the melting temperature of the alloy of the non-Au catalyst and group III material is high (note that there is no relatively low-temperature eutectic point in this alloy system).

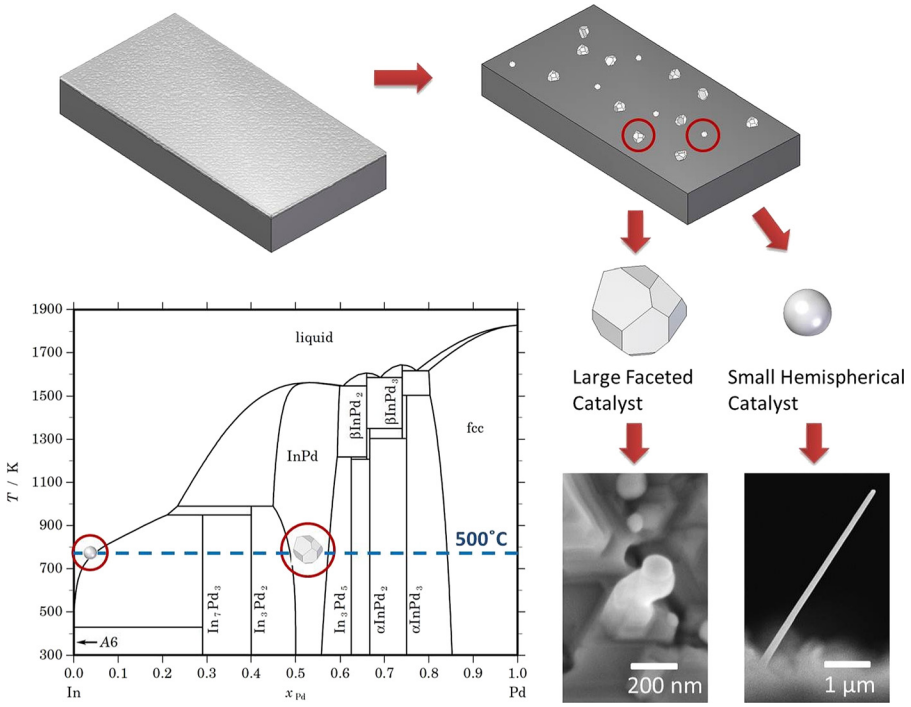

FIG. 4. Schematic illustration of the growth mechanisms of the Pd-catalyzed InAs nanostructures. Due to smaller catalyst size and high In concentration in the catalyst during the growth, InAs nanowires grow via the VLS mechanism. The larger catalysts induce InAs nanorods via the VSS mechanism. In the In-Pd phase diagram, the growth temperature of 500 °C is marked and both catalyst types are marked.

To understand why nanowires are induced by smaller Pd catalysts via the VLS mechanism and why nanorods are induced by larger Pd catalysts via the VSS mechanism, we note three factors. (1) The flat liquid/solid interface of a small Pd catalyst and its underlying nanowire is energetically favorable to be the nucleation site for the nanowire growth, while the nucleation at the solid/solid interface is more difficult.[37] (2) The catalysts with a higher group III concentration provide a rapid group III transportation during the one-dimensional nanostructures when compared to that of the larger solid catalysts. (3) Smaller catalysts often lead fast growth of one-dimensional nanostructures than larger catalysts do.[38] As a consequence, the growth of thin nanowires and thick nanorods is due to the synergetic effects of these factors.

In summary, the co-existence of VLS and VSS growths of one-dimensional InAs nanostructures catalyzed by thin Pd film in a MOCVD reactor has been identified. It was found the size of the catalysts plays a key role in determining the growth modes of the nanostructures. Small catalysts were found to promote InAs nanowire growth via the VLS growth model, while larger catalysts promote randomly oriented InAs nanorod growth via the VSS growth model. This study indicates that not only eutectic temperature of the catalysts is important in promoting VLS III-V nanowire growth but the concentration of group III material in the catalyst during growth can also lead the formation of liquid catalysts to promote VLS growth.

This research was supported by the Australian Research Council. The Australian National Fabrication Facility and Australian Microscopy and Microanalysis Research Facility, both established under the Australian Government's National Collaborative Research Infrastructure Strategy, are gratefully acknowledged for providing access to the facilities used in this work.

[1]H. Xia, Z. Y. Lu, T. X. Li, P. Parkinson, Z. M. Liao, F. H. Liu, W. Lu, W. D. Hu, P. P. Chen, H. Y. Xu, J. Zou, and C. Jagadish, ACS Nano **6**, 6005 (2012).
[2]J. Wallentin, N. Anttu, D. Asoli, M. Huffman, I. Aberg, M. H. Magnusson, G. Siefer, P. Fuss-Kailuweit, F. Dimroth, B. Witzigmann, H. Q. Xu, L. Samuelson, K. Deppert, and M. T. Borgstrom, Science **339**, 1057 (2013).
[3]E. Halpern, G. Elias, A. V. Kretinin, H. Shtrikman, and Y. Rosenwaks, Appl. Phys. Lett. **100**, 262105 (2012).
[4]I. Vurgaftman, J. R. Meyer, and L. R. Ram-Mohan, J. Appl. Phys. **89**, 5815 (2001).
[5]J. S. Blakemore, J. Appl. Phys. **53**, R123 (1982).
[6]J. Y. Marzin, J. M. Gerard, A. Izrael, D. Barrier, and G. Bastard, Phys. Rev. Lett. **73**, 716 (1994).
[7]M. S. Gudiksen, L. J. Lauhon, J. Wang, D. C. Smith, and C. M. Lieber, Nature **415**, 617 (2002).
[8]Y. N. Guo, H. Y. Xu, G. J. Auchterlonie, T. Burgess, H. J. Joyce, Q. Gao, H. H. Tan, C. Jagadish, H. B. Shu, X. S. Chen, W. Lu, Y. Kim, and J. Zou, Nano Lett. **13**, 643 (2013).
[9]M. Paladugu, J. Zou, Y. N. Guo, X. Zhang, Y. Kim, H. J. Joyce, Q. Gao, H. H. Tan, and C. Jagadish, Appl. Phys. Lett. **93**, 101911 (2008).
[10]S. Paiman, Q. Gao, H. H. Tan, C. Jagadish, K. Pemasiri, M. Montazeri, H. E. Jackson, L. M. Smith, J. M. Yarrison-Rice, X. Zhang, and J. Zou, Nanotechnology **20**, 225606 (2009).
[11]H. J. Joyce, Q. Gao, H. H. Tan, C. Jagadish, Y. Kim, X. Zhang, Y. N. Guo, and J. Zou, Nano Lett. **7**, 921 (2007).
[12]S. A. Dayeh, E. T. Yu, and D. Wang, Nano Lett. **7**, 2486 (2007).
[13]Z. M. Liao, Z. G. Chen, Z. Y. Lu, H. Y. Xu, Y. N. Guo, W. Sun, Z. Zhang, L. Yang, P. P. Chen, W. Lu, and J. Zou, Appl. Phys. Lett. **102**, 063106 (2013).
[14]C. Thelander, P. Caroff, S. Plissard, A. W. Dey, and K. A. Dick, Nano Lett. **11**, 2424 (2011).
[15]H. Y. Xu, Y. Wang, Y. N. Guo, Z. M. Liao, Q. Gao, N. Jiang, H. H. Tan, C. Jagadish, and J. Zou, Cryst. Growth Des. **12**, 2018 (2012).
[16]M. Paladugu, J. Zou, Y. N. Guo, G. J. Auchterlonie, H. J. Joyce, Q. Gao, H. H. Tan, C. Jagadish, and Y. Kim, Small **3**, 1873 (2007).
[17]H. J. Joyce, Q. Gao, H. H. Tan, C. Jagadish, Y. Kim, M. A. Fickenscher, S. Perera, T. B. Hoang, L. M. Smith, H. E. Jackson, J. M. Yarrison-Rice, X. Zhang, and J. Zou, Nano Lett. **9**, 695 (2009).
[18]K. A. Dick, P. Caroff, J. Bolinsson, M. E. Messing, J. Johansson, K. Deppert, L. R. Wallenberg, and L. Samuelson, Semicond. Sci. Technol. **25**, 024009 (2010).
[19]P. Caroff, K. A. Dick, J. Johansson, M. E. Messing, K. Deppert, and L. Samuelson, Nat. Nanotechnol. **4**, 50 (2009).
[20]P. Kratzer, S. Sakong, and V. Pankoke, Nano Lett. **12**, 943 (2012).
[21]Y. M. Shao, T. X. Nie, Z. M. Jiang, and J. Zou, Appl. Phys. Lett. **101**, 053104 (2012).

[22]P. A. Lin, D. Liang, S. Reeves, X. P. A. Gao, and R. M. Sankaran, Nano Lett. **12**, 315 (2012).
[23]Y. C. Chou, C. Y. Wen, M. C. Reuter, D. Su, E. A. Stach, and F. M. Ross, ACS Nano **6**, 6407 (2012).
[24]Y. W. Wang, V. Schmidt, S. Senz, and U. Gosele, Nat. Nanotechnol. **1**, 186 (2006).
[25]B. M. Kayes, M. A. Filler, M. C. Putnam, M. D. Kelzenberg, N. S. Lewis, and H. A. Atwater, Appl. Phys. Lett. **91**, 103110 (2007).
[26]S. Heun, B. Radha, D. Ercolani, G. U. Kulkarni, F. Rossi, V. Grillo, G. Salviati, F. Beltram, and L. Sorba, Small **6**, 1935 (2010).
[27]H. Xu, Y. Wang, Y. Guo, Z. Liao, Q. Gao, H. H. Tan, C. Jagadish, and J. Zou, Nano Lett. **12**, 5744 (2012).
[28]R. S. Wagner and W. C. Ellis, Appl. Phys. Lett. **4**, 89 (1964).
[29]P. W. Voorhees, J. Stat. Phys. **38**, 231 (1985).
[30]H. Okamoto, J. Phase Equilib. **24**, 481 (2003).
[31]H. Y. Xu, Y. N. Guo, W. Sun, Z. M. Liao, T. Burgess, H. F. Lu, Q. Gao, H. H. Tan, C. Jagadish, and J. Zou, Nanoscale Res. Lett. **7**, 589 (2012).
[32]Y. W. Chen, W. G. Wang, and S. H. Zhou, Mater. Lett. **65**, 2649 (2011).
[33]O. Oyelaran, T. Novet, C. D. Johnson, and D. C. Johnson, J. Am. Chem. Soc. **118**, 2422 (1996).
[34]A. K. Sra and R. E. Schaak, J. Am. Chem. Soc. **126**, 6667 (2004).
[35]J. R. Knight and D. W. Rhys, J. Less-Common Met. **1**, 292 (1959).
[36]A. I. Persson, M. W. Larsson, S. Stenstrom, B. J. Ohlsson, L. Samuelson, and L. R. Wallenberg, Nature Mater. **3**, 677 (2004).
[37]N. Wang, Y. Cai, and R. Q. Zhang, Mater. Sci. Eng. R **60**, 1 (2008).
[38]L. E. Froberg, W. Seifert, and J. Johansson, Phys. Rev. B **76**, 153401 (2007).